Supramolecular Photovoltaic Cells Based on Composite Molecular Nanoclusters: Dendritic Porphyrin and C_{60}, Porphyrin Dimer and C_{60}, and Porphyrin−C_{60} Dyad

Taku Hasobe,[†,‡] Prashant V. Kamat,[*,‡] Mark A. Absalom,[§] Yukiyasu Kashiwagi,[†] Joseph Sly,[§] Maxwell J. Crossley,[*,§] Kohei Hosomizu,[||] Hiroshi Imahori,[*,||] and Shunichi Fukuzumi[*,†]

Department of Material and Life Science, Graduate School of Engineering, Osaka University, CREST, Japan Science and Technology Agency (JST), Suita, Osaka 565-0871, Japan, Radiation Laboratory and Department of Chemical & Biomolecular Engineering, University of Notre Dame, Notre Dame, Indiana 46556-0579, School of Chemistry, The University of Sydney, New South Wales 2006, Australia, Department of Molecular Engineering, Graduate School of Engineering, Kyoto University, PRESTO, Japan Science and Technology Agency (JST), Katsura, Nishikyo-ku, Kyoto 615-8510, Japan, and Fukui Institute for Fundamental Chemistry, Kyoto University, 34-4, Takano-Nishihiraki-cho, Sakyo-ku, Kyoto 606-8103, Japan

Received: April 12, 2004; In Final Form: June 9, 2004

Novel organic solar cells have been prepared using molecular clusters of porphyrin dendrimer (donor) and fullerene (acceptor) dye units assembled on SnO_2 electrodes. The molecular clusters of porphyrin with dendritic structure and fullerene exhibit controlled size and shape in contrast with the reference systems (a porphyrin dimer and a porphyrin−fullerene dyad) without dendritic structure in TEM images, which show rather irregular and smaller clusters. The composite molecular nanoclusters of dendritic porphyrin and fullerene prepared in acetonitrile/toluene mixed solvent absorb light over entire spectrum of visible light. The comparison of photoelectrochemical properties of composite molecular cluster of porphyrin and fullerene with that of molecular cluster of porphyrin−C_{60} dyad with covalent linkage shows the importance of interpenetrating structure in each network to transport hole and electron efficiently. Furthermore, organic photovoltaic cells using clusters of supramolecular complexes of V-shaped porphyrin dimer and porphyrin dendrimers with fullerene exhibit remarkable enhancement in the photoelectrochemical performance as well as broader photoresponse in the visible and near-infrared regions as compared with the reference system. This clearly indicates that the $\pi-\pi$ interaction between porphyrins and fullerenes in the supramolecular clusters plays an important role in improving the light energy conversion efficiency.

Introduction

The requirement to develop inexpensive renewable energy sources has stimulated new approaches for production of efficient, low-cost organic photovoltaic devices.[1−6] Particular attention has been drawn in the recent year toward developing bulk heterojunction organic solar cells, which possess an active layer of a conjugated donor polymer and an acceptor fullerene.[7,8] Fullerene is suitable as an electron-acceptor component in such organic solar cells since electron-transfer reduction of C_{60} is highly efficient because of the minimal changes of structure and solvation associated with the electron-transfer reduction.[9−16] Thus, in these polymer blends, efficient photoinduced electron transfer occurs at the donor−fullerene interface, and intimate mixing of donor and fullerene acceptor is essential for efficient charge separation.

On the other hand, porphyrins have been involved as a chromophore and an electron donor in a number of important biological electron-transfer systems including the primary photochemical reactions of chlorophylls in the photosynthetic reaction centers.[17] Porphyrins contain an extensively conjugated two-dimensional π-system and are thereby suitable not only for synthetic light-harvesting systems[18,19] but also for efficient electron transfer because the uptake or release of electrons results in minimal structural and solvation change upon electron transfer.[20] In addition, rich and extensive absorption features of porphyrinoid systems guarantee increased absorption cross-sections and an efficient use of the solar spectrum.[21] In purple photosynthetic bacteria, visible light is harvested efficiently by the antenna complexes, which include a wheel-like array of chlorophylls.[22] In this context, porphyrin dendrimers are good candidates as light collectors since the antenna function of porphyrin dendrimers resembles that of the light harvesting antenna.[23,24] Moreover, porphyrins and fullerenes are known to form supramolecular complexes, which contain closest contacts between one of the electron-rich 6:6 bonds of the guest fullerene and the geometric center of the host porphyrin.[25−31] The porphyrin−fullerene interaction energies are reported to be in the range from −16 to −18 kcal mol^{-1}.[32] Such a strong interaction between porphyrins and fullerenes is likely to be a good driving force for the formation of supramolecular complexes between porphyrin and C_{60}. Thus, a combination of porphyrin dendrimers (chromophores and electron donor) and fullerenes (electron acceptor) seems ideal for fulfilling an enhanced light-harvesting efficiency of chromophores throughout the solar spectrum and a highly efficient conversion of the harvested light into the high energy state of the charge separation by photoinduced electron transfer.[33] We have previously reported composite clusters of porphyrin and fullerene in a mixture of polar and nonpolar solvents and assembling them

* Authors to whom correspondence should be addressed.
† Osaka University.
‡ University of Notre Dame.
§ The University of Sydney.
|| Kyoto University.

10.1021/jp048404r CCC: $27.50
Published on Web 08/04/2004

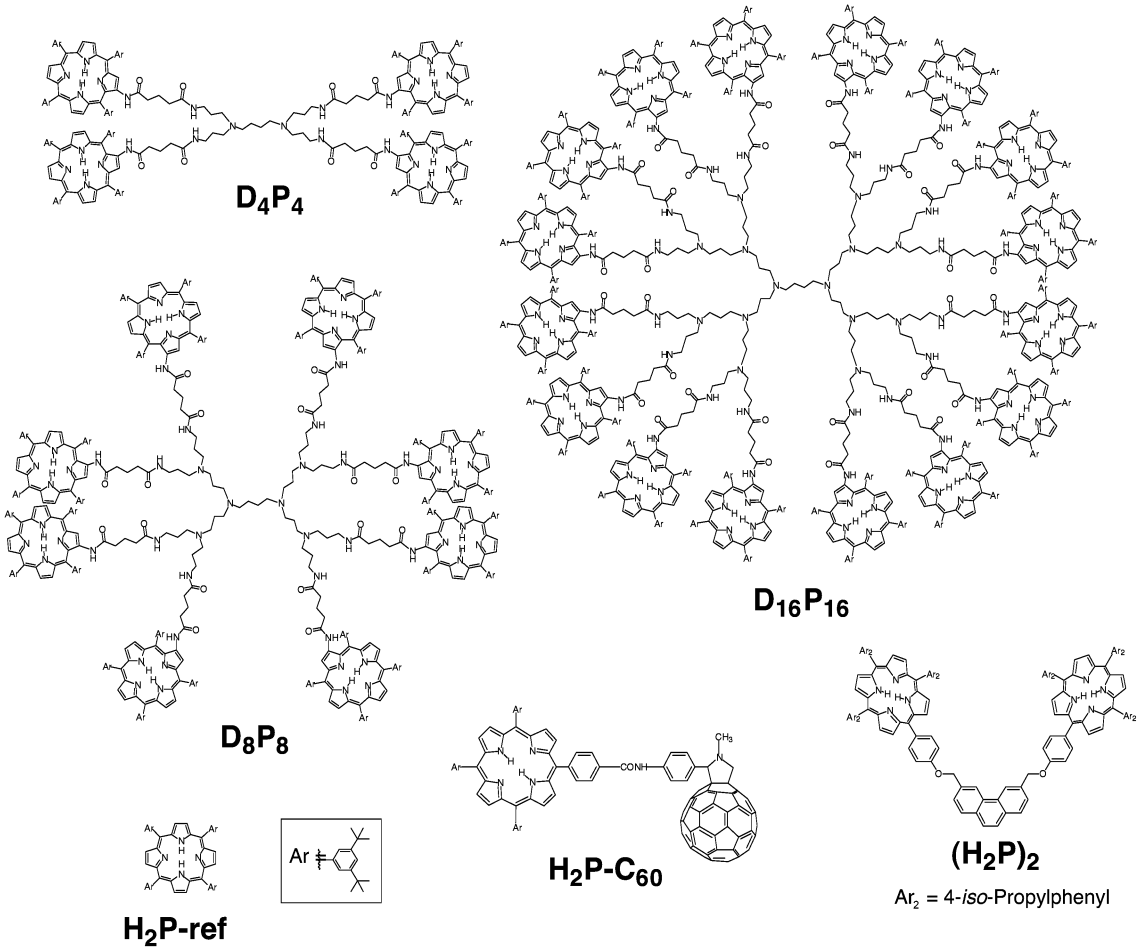

Figure 1. Porphyrin dendrimers and the reference compound employed in this study.

on a nanostructured SnO_2 electrode using an electrophoretic deposition technique.[34] The results clearly show the photoelectrochemical properties of composite systems of porphyrin and fullerene are superior to those of the single component. There are two essential factors to improve efficiency of the photocurrent generation in the composite systems. One is the charge-separation efficiency between porphyrin radical cation and fullerene radical anion, and the other is the efficiency of hole and electron transport in the thin film because of the multilayer.

We report herein a new type of solar cells composed of molecular clusters of porphyrin dendrimer (donor) and fullerene (acceptor) dye units assembled on SnO_2 electrodes, which have high charge-separation efficiency between porphyrin radical cation and fullerene radical anion as well as the efficient hole and electron transport. The porphyrin dendrimers (D_nP_n, n = 4, 8, 16), V-shaped porphyrin dimer [$(H_2P)_2$], and a porhyrin−C_{60} dyad (H_2P-C_{60}) employed in this study are shown in Figure 1 together with the reference porphyrin compound (H_2P-ref). They are used to prepare the porphyrin and C_{60} composite SnO_2 electrodes. Different molecular assemblies between porphyrin and C_{60} make it possible to control three-dimensional molecular structure, which is essential for efficient light energy conversion.

Experimental Section

Materials. Preparation of $(H_2P)_2$, H_2P-C_{60}, and H_2P-ref has been described elsewhere.[35] The porphyrin dendrimers were made by coupling of the porphyrin activated ester 5-{amino-2-[5,10,15,20-tetrakis(3,5-di-*tert*-butylphenyl)]-5-oxopentanoic acid 2,5-dioxopyrrolidin-1-yl ester (used in 10% excess) with the appropriate first, second, or third generation polypropylenimine dendrimer. The compounds were allowed to react in dichloromethane/triethylamine (10:1) mixed solvent, and the dendritic product was isolated by washing the organic solvent with water, drying it over sodium sulfate, evaporation to dryness, and chromatography over a Biobead SX-1 size exclusion column (200 cm × 3 cm) using toluene as the liquid phase and elution at 10 mL/h. Upon vigorous drying of the product, yields of fully coupled porphyrin−dendrimer are slightly higher than 80%. Spectroscopic data and MALDI-TOF spectra are fully consistent with the D_4P_4, D_8P_8, and $D_{16}P_{16}$ structures of the respective products.

Preparation of Clusters and Deposition onto OTE/SnO_2 Electrode. D_nP_n, H_2P-ref, and C_{60} are readily soluble in nonpolar solvents such as toluene. In mixed solvents, however, they aggregate to form large size clusters of diameter 100−300 nm. Since the aggregates are negatively charged under applied voltage, they can be electrophoretically deposited onto positive electrode.

Nanostructured SnO_2 films were cast on an optically transparent electrode (OTE) by applying a dilute (1−2%) colloidal solution (Alfa Chemicals) followed by annealing the dried film at 673 K. Details about the electrode preparation and its properties have been described elsewhere.[36] These films are highly porous and are electrochemically active to conduct charges across the film. The SnO_2 film electrode (OTE/SnO_2) and an OTE plate were introduced in a 1 cm path length cuvette and were connected to positive and negative terminals of the power supply, respectively. A known amount (∼2 mL) of the

cluster solution in acetonitrile/toluene (3/1, v/v) was transferred to a cuvette in which the two electrodes (viz., OTE/SnO_2 and OTE) were kept at a distance of ~6 mm using Teflon spacer. A dc voltage (500 V) was applied between these two electrodes using Fluke 415 power supply. The deposition of the film can be visibly seen as the solution becomes colorless with simultaneous black coloration of the OTE/SnO_2 electrode.

The UV−visible spectra were recorded on a Shimadzu 3101 spectrophotometer. Transmission electron micrographs (TEM) of the clusters were recorded by applying a drop of the sample to carbon-coated copper grid. Images were recorded using a Hitachi H600 transmission electron microscope. AFM measurements were carried out using a Nanoscope IIIa (Digital Instruments, Santa Barbara, CA) in the tapping mode.

Photoelectrochemical Measurements. The photoelectrochemical measurements were carried out with a standard two-compartment cell consisting of a working electrode and a Pt wire gauze counter electrode containing 0.5 M NaI and 0.01 M I_2 in acetonitrile as the electrolyte. Photocurrent measurements were made with a Keithley model 617 programmable electrometer. A collimated light beam from a 150 W xenon lamp with a 400 nm cutoff filter was used for excitation of the thin films cast on SnO_2 electrodes. A Bausch and Lomb high-intensity grating monochromator was introduced into the path of the excitation beam for the selected wavelength. The IPCE (incident photon-to-photocurrent efficiency) values were calculated by normalizing the photocurrent values for incident light energy and intensity and using the expression: IPCE (%) = $100 \times 1240 \times I_{sc}/(W_{in} \times \lambda)$, where I_{sc} is the short circuit photocurrent (A/cm^2), W_{in} is the incident light intensity (W/cm^2), and λ is the excitation wavelength (nm). The fill factor (FF) is defined as FF = $[I \times V]_{max}/(I_{sc} \times V_{oc})$, where V_{oc} is open circuit photovoltage. Overall power conversion efficiency (η) is determined as $\eta = FF \times I_{sc} \times V_{oc}/W_{in}$.

Result and Discussion

Porphyrin dendrimers (D_nP_n) and V-shaped porphyrin dimer $(H_2P)_2$ form supramolecular complexes with fullerene molecules in toluene, and they are clusterized in an acetonitrile/toluene mixed solvent system. Then, the clusters are attached on nanostructured SnO_2 electrodes by an electrophoretic deposition method (500 V for 1 min) as reported previously.[34,37,38] The organization of D_nP_n and C_{60} composite clusters [denoted as $(D_nP_n+C_{60})_m$ ($n = 4, 8, 16$)] was performed by injecting a mixed toluene solution of D_nP_n, $(H_2P)_2$ and C_{60} into acetonitrile/toluene (3/1, v/v). Herein the concentration of one porphyrin unit in these composite clusters is taken as the same in the dendrimers: $[D_4P_4] = 0.048$ mM, $[D_8P_8] = 0.024$ mM, $[D_{16}P_{16}] = 0.012$ mM, $[(H_2P)_2] = 0.13$ mM, and [H2P-ref] = 0.19 mM in acetonitrile/toluene (3/1, v/v) whereas the concentration of C_{60} (0.31 mM) is in excess of the concentration of one porphyrin unit in acetonitrile/toluene (3/1, v/v). This procedure allows us to achieve the supramolecular complex formation between D_nP_n and C_{60} and the clusterization at the same time. The clusterization of porphyrin and C_{60} reference system without the dendritic structure [denoted as $(H_2P\text{-ref}+C_{60})_m$] was also performed using the same approach.[34,37,38]

The absorption spectra of $(D_nP_n+C_{60})_m$ and $(H_2P\text{-ref}+C_{60})_m$ in acetonitrile/toluene 3:1 mixture are much broader than those in toluene, indicating formation of the clusters in the mixed solvent (Figure 2A). The broad long-wavelength absorption in the 700−800 nm region is diagnostic of the charge-transfer absorption band due to the π-complex formed between the porphyrin and C_{60} since similar charge-transfer interactions

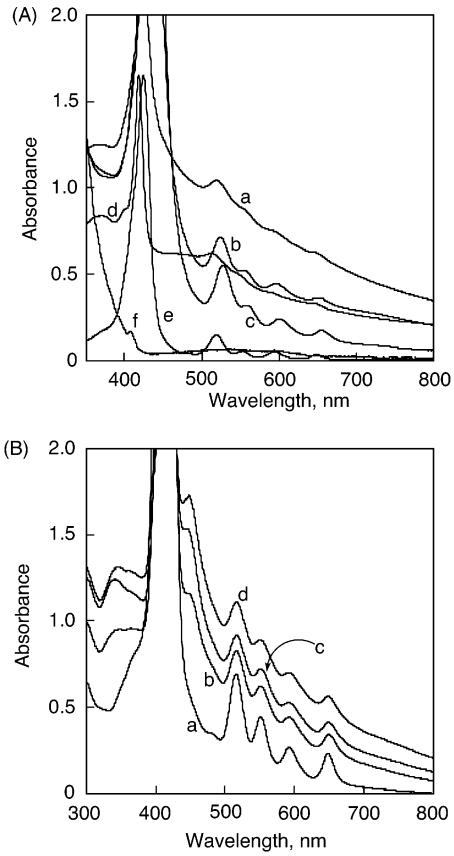

Figure 2. (A) Absorption spectra of (a) $(D_4P_4+C_{60})_m$ ($[D_4P_4] = 0.048$ mM, $[C_{60}] = 0.31$ mM), (b) $(D_8P_8+C_{60})_m$ ($[D_8P_8] = 0.024$ mM, $[C_{60}] = 0.31$ mM), (c) $(D_{16}P_{16}+C_{60})_m$ ($[D_{16}P_{16}] = 0.012$ mM, $[C_{60}] = 0.31$ mM), and (d) $(H_2P\text{-ref}+C_{60})_m$ ([H2P-ref] = 0.19 mM, $[C_{60}] = 0.31$ mM) in acetonitrile/toluene (3/1, v/v), (e) 4.1 μM $D_{16}P_{16}$, and (f) 150 μM C_{60} in toluene. (B) Absorption spectra of $((H_2P)_2+C_{60})_m$ ($[(H_2P)_2] = 0.13$ mM; (a) $[C_{60}] = 0$ mM, (b) $[C_{60}] = 0.06$ mM, (c) $[C_{60}] = 0.13$ mM, and (d) $[C_{60}] = 0.31$ mM) in acetonitrile/toluene (3/1, v/v).

leading to extended absorption have been observed for porphyrin−C_{60} dyads linked at close proximity.[35c,39,40]

Figure 2B shows the absorption spectra of $((H_2P)_2+C_{60})_m$ in acetonitrile/toluene 3:1 mixture with different concentrations of C_{60}. The absorption becomes larger and broader with increasing concentration of C_{60}. This may also result from strong $\pi-\pi$ interaction between porphyrin and fullerene.[35c,39,40]

The TEM images of $(D_4P_4+C_{60})_m$ (Figure 3A) and $(D_8P_8+C_{60})_m$ (Figure 3B) show formation of large nanoclusters of diameter 200−300 nm with well-controlled size and shape. This is in sharp contrast to the clusters of $(D_{16}P_{16}+C_{60})_m$ and $(H_2P\text{-ref}+C_{60})_m$, the TEM images of which show rather irregular and smaller clusters (Figure 3C,E). These results indicate that dendritic structure plays an important role in controlling the formation of the molecular clusters. In the case of $D_{16}P_{16}$, however, the steric crowdness of 16 porphyrin molecules may preclude effective interaction between porphyrin and C_{60} to form the molecular clusters. Judging from the molecular scale of D_8P_8 (3.5 nm—determined from diffusion studies) and C_{60}, we can conclude that D_8P_8 molecules are self-assembled with C_{60} molecules in the mixed solution to yield large donor−acceptor assembled nanoclusters with an interpenetrating network. On the other hand, strong aggregation of $((H_2P)_2+C_{60})_m$ is observed in Figure 3D. This may be ascribed to strong interaction between V-shaped porphyrin and fullerene. The size and shape of molecular cluster using porphyrin and fullerene is largely dependent on the structure of porphyrin.

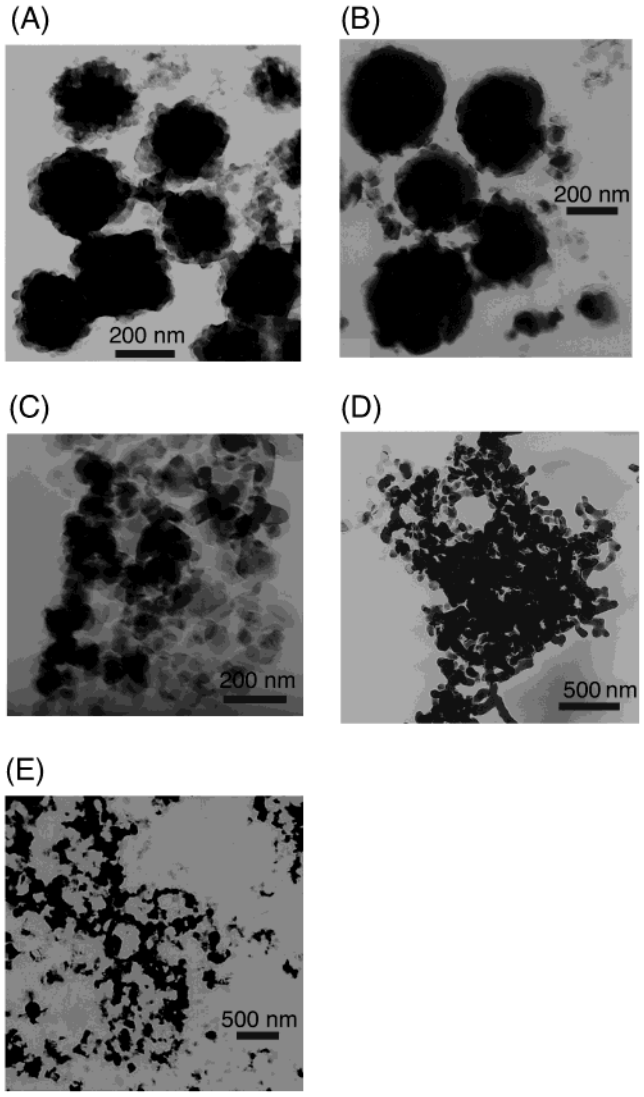

Figure 3. TEM images of (A) $(D_4P_4+C_{60})_m$ ($[D_4P_4] = 0.048$ mM, $[C_{60}] = 0.31$ mM); (B) $(D_8P_8+C_{60})_m(D_8P_8+C_{60})_m$ ($[D_8P_8] = 0.024$ mM, $[C_{60}] = 0.31$ mM); (C) $(D_{16}P_{16}+C_{60})_m$ ($[D_{16}P_{16}] = 0.012$ mM, $[C_{60}] = 0.31$ mM); (D) $((H_2P)_2+C_{60})_m$ ($[(H_2P)_2] = 0.13$ mM, $[C_{60}] = 0.31$ mM); and (E) $(H_2P\text{-ref}+C_{60})_m$ ($[H_2P\text{-ref}] = 0.19$ mM, $[C_{60}] = 0.31$ mM) in acetonitrile/toluene = 3/1.

Upon subjecting the resultant cluster suspension to a high electric dc field (500 V for 1 min), mixed D_nP_n and C_{60} clusters $[(D_nP_n+C_{60})_m]$, mixed $(H_2P)_2$ and C_{60} clusters $[((H_2P)_2+C_{60})_m]$, and reference clusters $[(H_2P\text{-ref}+C_{60})_m]$ were deposited onto an optically transparent electrode (OTE) of a nanostructured SnO_2 electrode (OTE/SnO_2) to give modified electrodes [denoted as OTE/SnO_2/$(D_nP_n+C_{60})_m$ ($n = 4$, 8, 16), (OTE/SnO_2/$((H_2P)_2+C_{60})_m$, and OTE/SnO_2/$(H_2P\text{-ref}+C_{60})_m$), respectively]. The absorptivity of the OTE/SnO_2/$(D_nP_n+C_{60})_m$ system is enhanced compared with that of clusters made from the nondendritic porphyrin reference compound (Figure 4A). These results ensure that the incident light is absorbed intensively in the visible and near-infrared regions by OTE/SnO_2/$(D_nP_n+C_{60})_m$. On the other hand, the absorption spectrum of OTE/SnO_2/$((H_2P)_2+C_{60})_m$ has higher absorption property with increasing concentration of C_{60} (Figure 4B). The absorption of OTE/SnO_2/$((H_2P)_2+C_{60})_m$ with a low concentration of C_{60} (0.06 mM, spectrum b) is much higher than that of OTE/SnO_2/$((H_2P)_2)_m$ without C_{60} (0 mM, spetrum a). Absorption of molecular clusters on OTE/SnO_2 is largely dependent on degree of aggregation.

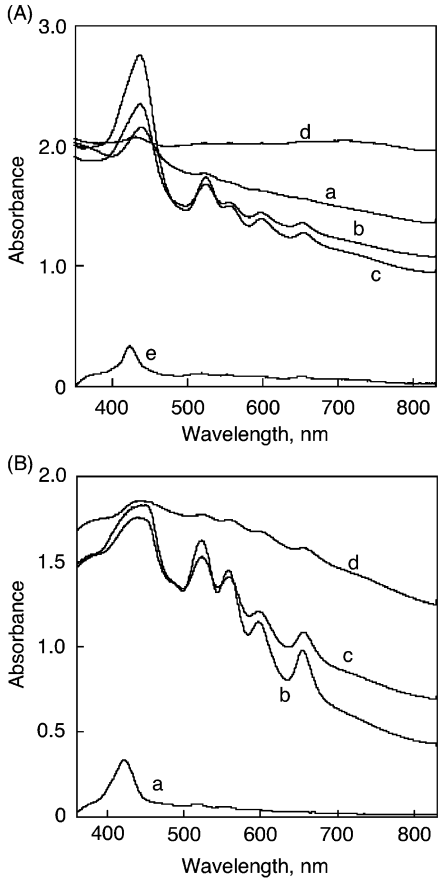

Figure 4. (A) Absorption spectra of OTE/SnO_2/$(D_nP_n+C_{60})_m$ electrodes (a: $n = 4$, b: $n = 8$, and c: $n = 16$), (d) OTE/SnO_2/$(H_2P\text{-ref}+C_{60})_m$, and (e) OTE/$SnO_2$/$(H_2P\text{-ref})_m$ systems; $[D_4P_4] = 0.048$ mM, $[D_8P_8] = 0.024$ mM, $[D_{16}P_{16}] = 0.012$ mM, and $[H_2P\text{-ref}] = 0.19$ mM; $[C_{60}] = 0.31$ mM in acetonitrile/toluene = 3/1. (B) Absorption spectra of OTE/SnO_2/$((H_2P)_2+C_{60})_m$ electrodes; $[(H_2P)_2] = 0.13$ mM; $[C_{60}]$ = (a) 0 mM, (b) 0.06 mM, (c) 0.13 mM, and (d) 0.31 mM.

The AFM image of OTE/SnO_2/$(D_4P_4+C_{60})_m$ reveals the cluster aggregation with a regular size (Figure 5A). The OTE/SnO_2/$(D_4P_4+C_{60})_m$ film is composed of closely packed clusters of about 100 nm size, whereas the cluster size of OTE/SnO_2/$((H_2P)_2+C_{60})_m$ film is slightly smaller. The cluster size in the AFM image is smaller than that observed in the TEM image of the composite clusters in acetonitrile/toluene (3/1, v/v). This indicates that slow evaporation of the solvent on the TEM grid is responsible for yielding a larger cluster size of $(D_4P_4+C_{60})_m$ and $((H_2P)_2+C_{60})_m$ in contrast to this quick deposition technique under the influence of a dc electric field.[34]

Photoelectrochemical measurements were performed with a standard two-electrode system consisting of a working electrode and a Pt wire gauze electrode in 0.5 M NaI and 0.01 M I_2 in air-saturated acetonitrile. First, we examined the effect of C_{60} on the photoelectrochemical properties of the OTE/SnO_2/$(H_2P\text{-ref}+C_{60})_m$ system.

The IPCE values increase with increasing C_{60} concentration (0−0.31 mM in acetonitrile/toluene) at a constant concentration of H_2P-ref (0.19 mM) as shown in Figure 6A. This indicates that an electron transfer from the excited state of porphyrin to C_{60} takes place leading to efficient photocurrent generation.[10,12−15,33,41−43] On the other hand, the IPCE value of porphyrin and fullerene dyad cluster system (OTE/SnO_2/$(H_2P-C_{60})_m$) is much lower than that of OTE/SnO_2/$(H_2P\text{-ref}+C_{60})_m$. In the case of organic solar cells composed of electron donor and acceptor molecules, the resulting hole and electron transport

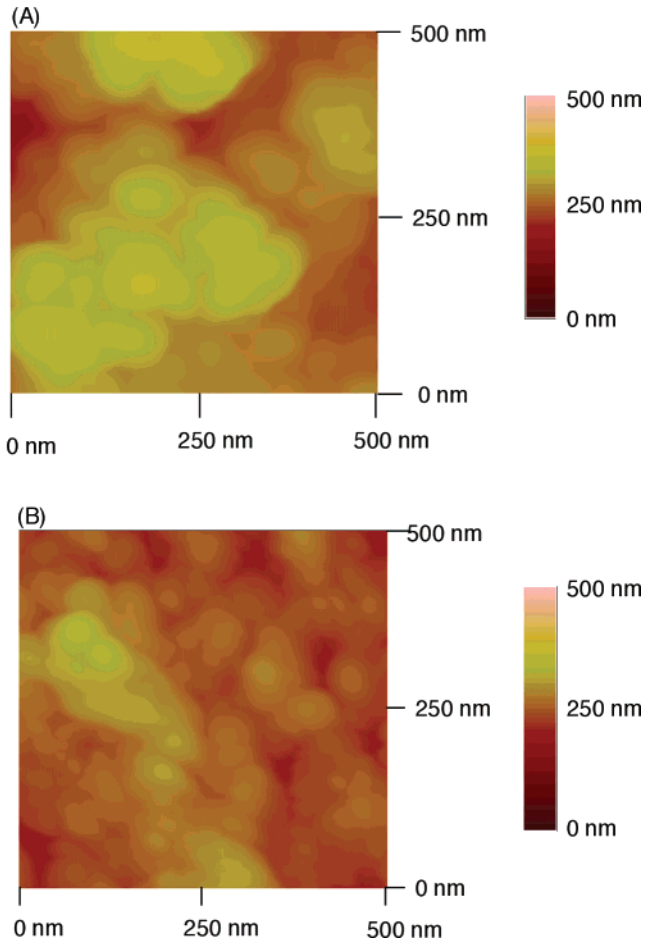

Figure 5. (A) AFM image of OTE/SnO_2/(D_4P_4+C_{60})$_m$ electrode, [D_4P_4] = 0.048 mM; [C_{60}] = 0.31 mM in acetonitrile/toluene = 3/1. (B) AFM image of OTE/SnO_2/((H_2P)$_2$+C_{60})$_m$ electrode; [(H_2P)$_2$] = 0.13 mM; [C_{60}] = 0.31 mM.

as well as charge separation between porphyrin and fullerene in the thin film are essential factors to improve efficiency of the photocurrent generation in the composite systems (vide supra). Fast self-exchange electron transfer of porphyrins and fullerenes in the molecular clusters with interpenetrating network in the thin film results in efficient hopping of hole and electron in each network.[44] In the case of OTE/SnO_2/(H_2P-ref+C_{60})$_m$, the absence of covalent bonding between porphyrin and fullerene enables to form interpenetrating structure in each network. In contrast, the covalent linkage in OTE/SnO_2/(H_2P−C_{60})$_m$ precludes formation of efficient interpenetrating structure.

Figure 7A shows the wavelength dependence of IPCE values of the OTE/SnO_2/((H_2P)$_2$+C_{60})$_m$ system with different concentrations of C_{60}. The IPCE values increase with increasing concentration of C_{60}, when the action spectra become broader in the visible and near-infrared region. The further increase of C_{60} (more than 0.31 mM) resulted in no increase in the IPCE value. Thus, the optimum concentration of C_{60} relative to the porphyrin moieties is determined as 0.31 mM. The action spectra indicate that the higher IPCE and the broader photoresponse are attained by using V-shaped porphyrin as compared with action spectrum of OTE/SnO_2/(H_2P-ref+C_{60})$_m$ (Figure 6A) because of efficient supramolecular complex formation between porphyrin and fullerene.[25−31]

Figure 7B shows the wavelength dependence of the incident photon-to-photocurrent efficiency (IPCE) of the OTE/SnO_2/(D_nP_n+C_{60})$_m$ system and the reference system (OTE/SnO_2/(H_2P-ref+C_{60})$_m$) at a constant concentration ratio of porphyrin to C_{60}

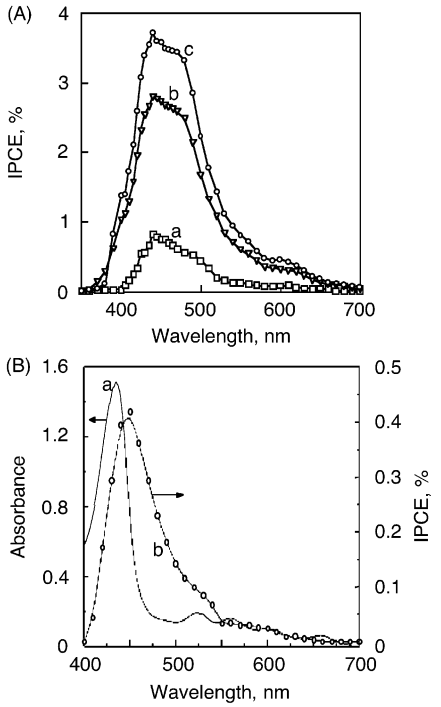

Figure 6. Photocurrent action spectra (IPCE vs wavelength) of (A) OTE/SnO_2/(H_2P-ref+C_{60})$_m$ electrodes ([H_2P-ref] = 0.19 mM; [C_{60}] = (a) 0 mM, (b) 0.19 mM, and (c) 0.31 mM in acetonitrile/toluene = 3/1.) (B) Absorption spectrum (a) of OTE/SnO_2/(H_2P−C_{60})$_m$ electrode and the photocurrent action spectra (IPCE vs wavelength) (b) Electrolyte: 0.5 M NaI and I_2 0.01 M I_2 in acetonitrile.

([D_4P_4] = 0.048 mM, [D_8P_8] = 0.024 mM, [$D_{16}P_{16}$] = 0.048 mM and [H_2P-ref] = 0.19 mM; [C_{60}] = 0.31 mM in acetonitrile/toluene 3:1 mixture). The OTE/SnO_2/(D_4P_4+C_{60})$_m$ system (a in Figure 7B) exhibits maximum IPCE value of 15% and broad photoresponse, which extends well into the infrared (up to 1000 nm) in contrast with the reference system (d in Figure 7B). The action spectra at the long wavelength region (e.g., the peak around 880 nm in Figure 7B) may result from the charge-transfer interaction of the porphyrins and C_{60}.[35c,39,40] Such an effective photoenergy conversion is ascribed to the dendritic structure that controls three-dimensional organization between porphyrin and C_{60}. However, the IPCE value decreases with increasing the number of dendrimer generation and the OTE/SnO_2/($D_{16}P_{16}$+C_{60})$_m$ system has even smaller IPCE values compared with the reference system [OTE/SnO_2/(H_2P-ref+C_{60})$_m$] (c in Figure 7B).

The IPCE values of OTE/SnO_2/((H_2P)$_2$+C_{60})$_m$ system of the V-shaped porphyrin dimer (d in Figure 7A) are rather similar to those of the OTE/SnO_2/(D_4P_4+C_{60})$_m$ system (a in Figure 7B). This indicates that insertion of C_{60} between two porphyrin rings of the V-shaped porphyrin dimer and the D_4P_4 dendrimer plays important role in the photocurrent generation (see Supporting Information S1 for the calculated structure of the V-shaped porphyrin dimer). The closest distance between a carbon of C_{60} and the center of the porphyrin ring has been determined as 2.856 Å by the X-ray crystal structure of the C_{60} complex with a jaw-like bis-porphyrin.[27a,29b] Thus, the smallest center-to-center distance of two porphyrin rings which can bite C_{60} is estimated as 12.8 Å by adding the diameter of C_{60} (7.1 Å) to twice of the closest distance between a carbon of C_{60} and the center of porphyrin ring (5.7 Å). The structure of (H_2P)$_2$ obtained by AM1 (Figure S1 in Suporting Information) has enough space to insert C_{60}. In the case of $D_{16}P_{16}$, however, the space between porphyrin rings may be too small for the interaction with C_{60}. This

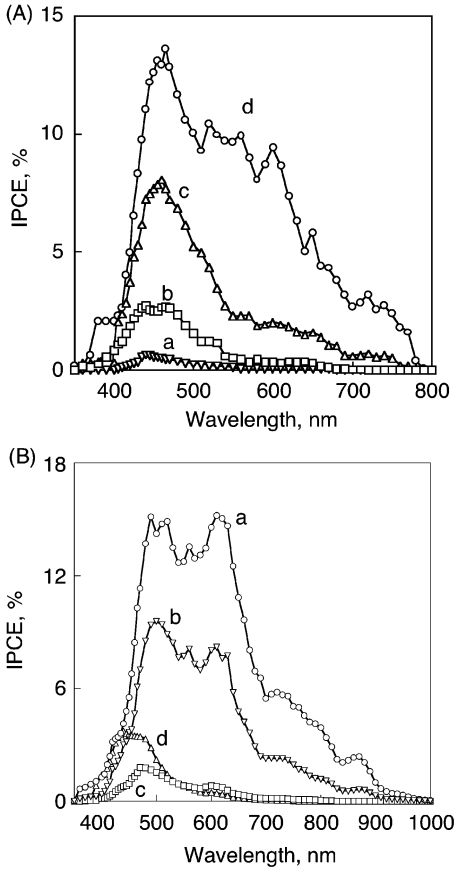

Figure 7. (A) Photocurrent action spectra (IPCE vs wavelength) of OTE/SnO_2/$((H_2P)_2+C_{60})_m$ electrodes; $(H_2P)_2$ = 0.13 mM; $[C_{60}]$ = (a) 0 mM, (b) 0.06 mM, (c) 0.13 mM, and (d) 0.31 mM. (B) Photocurrent action spectra (IPCE vs wavelength) of OTE/SnO_2/$(D_nP_n+C_{60})_m$ electrodes; $[C_{60}]$ = 0.31 mM in acetonitrile/toluene = 3/1; (a) $[D_4P_4]$ = 0.048 mM, (b) $[D_8P_8]$ = 0.024 mM, (c) $[D_{16}P_{16}]$ = 0.012 mM, and (d) $[H_2P\text{-ref}]$ = 0.19 mM. Electrolyte: 0.5 M NaI and I_2 0.01 M I_2 in acetonitrile.

indicates that supramolecular assembly between electron donor and acceptor is very important in construction of light energy conversion system, whereas the distance between porphyrins is an essential factor to form such a supramolecular complex.

The photocurrent and photovoltage responses recorded following the excitation of OTE/SnO_2/$((H_2P)_2+C_{60})_m$ electrode in the visible light region (λ > 400 nm) are shown in Figure 8, panels A and B, respectively. The photocurrent response is prompt, steady, and reproducible during repeated on/off cycles of the visible light illumination. The short circuit photocurrent density (I_{sc} = 0.14 mA/cm^2) and open circuit voltage (V_{oc} = 230 mV) were obtained reproducibly during these measurements. Blank experiments conducted with OTE/SnO_2 (i.e., by excluding composite clusters $((H_2P)_2+C_{60})_m$ produced no detectable photocurrent under the similar experimental conditions. These experiments confirmed the role of $((H_2P)_2+C_{60})_m$ assembly toward harvesting light energy and generating photocurrent during the operation of a photoelectrochemical cell. Similar photoresponses were obtained for the OTE/SnO_2/$(D_nP_n+C_{60})_m$ systems.

Figure 9 shows current−voltage (*I*/*V*) characteristics of the OTE/SnO_2/$(D_4P_4+C_{60})_m$, OTE/SnO_2/$((H_2P)_2+C_{60})_m$, and OTE/SnO_2/$(H_2P\text{-ref}+C_{60})_m$ systems under visible light irradiation (λ > 400 nm). The OTE/SnO_2/$(D_4P_4+C_{60})_m$ system has a FF of 0.31, open circuit voltage (V_{oc}) of 220 mV, short circuit current density (I_{sc}) of 0.29 mA cm^{-2}, and the overall power conversion

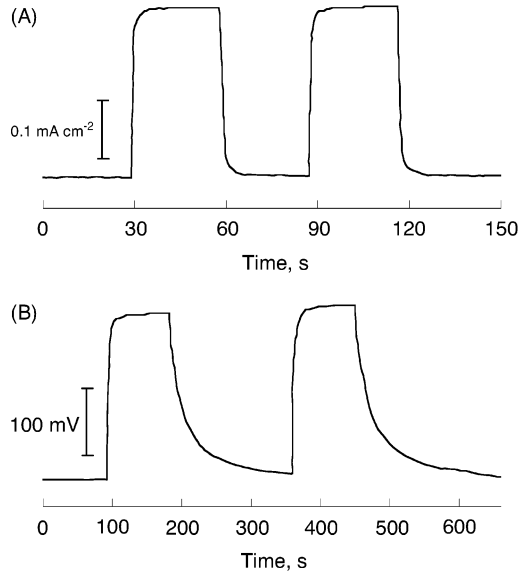

Figure 8. (A) Photocurrent response and (B) photovoltage response of OTE/SnO_2/$((H_2P)_2+C_{60})_m$ electrode prepared from cluster solution of $([(H_2P)_2]$ = 0.13 mM; $[C_{60}]$ = 0.31 mM to visible light illumination (λ > 400 nm); electrolyte: 0.5 M NaI and I_2 0.01 M I_2 in acetonitrile; input power 6.2 mW/cm^2.

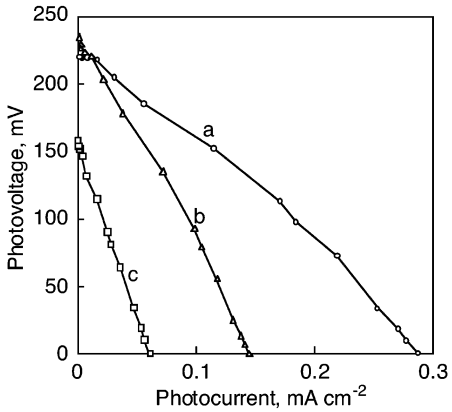

Figure 9. Current-voltage (*I*/*V*) characteristics of (a) OTE/SnO_2/$(D_4P_4+C_{60})_m$, (b) OTE/SnO_2/$((H_2P)_2+C_{60})_m$, and (c) OTE/SnO_2/$(H_2P\text{-ref}+C_{60})_m$ electrodes. Electrolyte: 0.5 M NaI and 0.01 M I_2 in acetonitrile; input power: 6.2 mW cm^{-2}, λ > 400 nm. $[D_4P_4]$ = 0.048 mM; $[(H_2P)_2]$ = 0.13 mM; $[H_2P\text{-ref}]$ = 0.19 mM; $[C_{60}]$ = 0.31 mM.

efficiency (η) of 0.32% at input power (W_{in}) of 6.2 mW cm^{-2}. Under the same conditions, η of the OTE/SnO_2/$((H_2P)_2+C_{60})_m$ system is 0.15%. The *I*/*V* characteristics of OTE/SnO_2/$(D_4P_4+C_{60})_m$ system is remarkably enhanced (about 10 times) in comparison with the OTE/SnO_2/$(H_2P\text{-ref}+C_{60})_m$ system (η = 0.035%) under the same experimental conditions.

Photocurrent generation in the present system is initiated by photoinduced electron transfer from the porphyrin excited singlet state ($^1H_2P^*/H_2P^{\bullet+}$ = −0.7 V vs NHE)[34] in the dendrimer to C_{60} ($C_{60}/C_{60}^{\bullet-}$ = −0.2 V vs NHE)[34] in the porphyrin dendrimer−C_{60} supramolecular complex rather than direct electron injection to conduction band of SnO_2 (0 V vs NHE) system. The reduced C_{60} injects electrons into the SnO_2 nanocrystallites, whereas the oxidized porphyrin ($H_2P/H_2P^{\bullet+}$ = 1.2 V vs NHE)[34] undergoes the electron-transfer reduction with the iodide (I_3^-/I^- = 0.5 V vs NHE)[34] in the electrolyte system.

In summary, we have constructed the various organic photovoltaic systems using molecular cluster assemblies of porphyrins (electron donor) and fullerene (electron acceptor)

and compared their photolectrochemical properties in detail. The comparison of the photoelectrochemical properties indicates that the composite clusters of V-shaped porphyrin dimer and porphyrin dendrimers with fullerene exhibit remarkable enhancement in the photoelectrochemical performance as well as broader photoresponse in the visible and near-infrared regions due to the effective $\pi-\pi$ interaction between porphyrins and fullerenes in the interpenetrating structure of the supramolecular clusters as compared with the reference system.

Acknowledgment. This work was partially supported by a Grant-in-Aid to S.F. (No. 13440216), a Grant-in-Aids for COE Research (Kyoto University Alliance for Chemistry) and Scientific Research (No. 16310073 to H.I.) from the Ministry of Education, Culture, Sports, Science and Technology, Japan. M.J.C. acknowledges generous funding of this research from the Australian Research Council. P.V.K. acknowledges the support from the Office of Basic Energy Science of the U.S. Department of the Energy. This is Contribution No. NDRL 4523 from the Notre Dame Radiation Laboratory and from Osaka University.

Supporting Information Available: Structure of $(H_2P)_2$ obtained by AM1 calculation. This material is available free of charge via the Internet at http://pubs.acs.org.

References and Notes

(1) (a) Hagfeldt, A.; Grätzel, M. *Acc. Chem. Res.* **2000**, *33*, 269. (b) Grätzel, M. *Nature* **2001**, *414*, 338. (c) Bignozzi, C. A.; Argazzi, R.; Kleverlaan, C. J. *Chem. Soc. Rev.* **2000**, *29*, 87.

(2) (a) Hagfeldt, A.; Grätzel, M. *Chem. Rev.* **1995**, *95*, 49. (b) Bonhôte, P.; Moser, J.-E.; Humphry-Baker, R.; Vlachopoulos, N.; Zakeeruddin, S. M.; Walder, L.; Grätzel, M. *J. Am. Chem. Soc.* **1999**, *121*, 1324. (c) Hagfeldt, A.; Grätzel, M. *Acc. Chem. Res.* **2000**, *33*, 269.

(3) (a) O'Regan, B.; Grätzel, M. *Nature* **1991**, *353*, 737. (b) Bach, U.; Lupo, D.; Comte, P.; Moser, J. E.; Weissörtel, F.; Salbeck, J.; Spreitzer, H.; Grätzel, M. *Nature* **1998**, *395*, 583.

(4) Cinnsealach, R.; Boschloo, G.; Rao, S. N.; Fitzmaurice, D. *Sol. Energy Mater. Sol. Cells* **1999**, *55*, 215.

(5) Shah, A.; Torres, P.; Tscharner, R.; Wyrsch, N.; Keppner, H. *Science* **1999**, *285*, 692.

(6) (a) Granström, M.; Petrisch, K.; Arias, A. C.; Lux, A.; Andersson, M. R.; Friend, R. H. *Nature* **1998**, *395*, 257. (b) Halls, J. J. M.; Walsh, C. A.; Greenham, N. C.; Marseglia, E. A.; Friend, R. H.; Moratti, S. C.; Holmes, A. B. *Nature* **1995**, *376*, 498.

(7) (a) Schmidt-Mende, L.; Fechtenkötter, A.; Müllen, K.; Moons, E.; Friend, R. H.; MacKenzie, J. D. *Science* **2001**, *293*, 1119. (b) Huynh, W. U.; Dittmer, J. J.; Alivisatos, A. P. *Science* **2002**, *295*, 2425.

(8) (a) Yu, G.; Gao, J.; Hummelen, J. C.; Wudl, F.; Heeger, A. J. *Science* **1995**, *270*, 1789. (b) Shaheen, S. E.; Brabec, C. J.; Sariciftci, N. S.; Padinger, F.; Fromherz, T.; Hummelen, J. C. *Appl. Phys. Lett.* **2001**, *78*, 841.

(9) (a) Padinger, F.; Rittberger, R. S.; Sariciftci, N. S. *Adv. Funct. Mater.* **2003**, *13*, 85. (b) Wienk, M. M.; Kroon, J. M.; Verhees, W. J. H.; Knol, J.; Hummelen, J. C.; van Hal, P. A.; Janssen, R. A. J. *Angew. Chem. Ind. Ed.* **2003**, *42*, 3371.

(10) (a) Fukuzumi, S.; Imahori, H. In *Electron Transfer in Chemistry*; Balzani, V., Ed.; Wiley-VCH: Weinheim, 2001; Vol. 2, pp 927−975. (b) Fukuzumi, S.; Guldi, D. M. In *Electron Transfer in Chemistry*; Balzani, V., Ed.; Wiley-VCH: Weinheim, 2001; Vo. 2, pp 270−337. (c) Imahori, H. *Org. Biomol. Chem.* **2004**, *2*, 1425.

(11) Guldi, D. M.; Kamat, P. V. In *Fullerenes, Chemistry, Physics, and Technology*; Kadish, K. M., Ruoff, R. S., Eds.; Wiley-Interscience: New York, 2000; pp 225−281.

(12) (a) Imahori, H.; Tamaki, K.; Guldi, D. M.; Luo, C.; Fujitsuka, M.; Ito, O.; Sakata, Y.; Fukuzumi, S. *J. Am. Chem. Soc.* **2001**, *123*, 2607. (b) Imahori, H.; Guldi, D. M.; Tamaki, K.; Yoshida, Y.; Luo, C.; Sakata, Y.; Fukuzumi, S. *J. Am. Chem. Soc.* **2001**, *123*, 6617.

(13) (a) Imahori, H.; Hagiwara, K.; Akiyama, T.; Aoki, M.; Taniguchi, S.; Okada, T.; Shirakawa, M.; Sakata, Y. *Chem. Phys. Lett.* **1996**, *263*, 545. (b) Tkachenko, N. V.; Guenther, C.; Imahori, H.; Tamaki, K.; Sakata, Y.; Fukuzumi, S.; Lemmetyinen, H. *Chem. Phys. Lett.* **2000**, *326*, 344.

(14) (a) Imahori, H.; Tamaki, K.; Yamada, H.; Yamada, K.; Sakata, Y.; Nishimura, Y.; Yamazaki, I.; Fujitsuka, M.; Ito, O. *Carbon* **2000**, *38*, 1599. (b) Vehmanen, V.; Tkachenko, N. V.; Imahori, H.; Fukuzumi, S.; Lemmetyinen, H. *Spectrochim. Acta, Part A* **2001**, *57*, 2229.

(15) (a) Imahori, H.; Yamada, H.; Guldi, D. M.; Endo, Y.; Shimomura, A.; Kundu, S.; Yamada, K.; Okada, T.; Sakata, Y.; Fukuzumi, S. *Angew. Chem., Int. Ed.* **2002**, *41*, 2344. (b) Imahori, H.; Tamaki, K.; Araki, Y.; Sekiguchi, Y.; Ito, O.; Sakata, Y.; Fukuzumi, S. *J. Am. Chem. Soc.* **2002**, *124*, 5165.

(16) Guldi, D. M.; Asmus, K.-D. *J. Am. Chem. Soc.* **1997**, *119*, 5744.

(17) (a) *The Photosynthetic Reaction Center*; Deisenhofer, J., Norris, J. R., Eds.; Academic Press: San Diego, 1993. (b) *Anoxygenic Photosynthetic Bacteria*; Blankenship, R. E., Madigan, M. T., Bauer, C. E., Eds.; Kluwer Academic Publishing: Dordrecht, The Netherlands, 1995.

(18) Harvey, P. D. In *The Porphyrin Handbook*; Kadish, K. M., Smith, K. M., Guilard, R., Eds.; Academic Press: San Diego, 2003; Vol. 18, pp 63−250.

(19) (a) Wagner, R. W.; Lindsey, J. S. *Pure Appl. Chem.* **1996**, *68*, 1373−1380. (b) Sazanovich, I. V.; Kirmaier, C.; Hindin, E.; Bocian, D. F.; Linsey, J. S.; Holten, D. *J. Am. Chem. Soc.* **2004**, *126*, 2664.

(20) (a) Fukuzumi, S. In *The Porphyrin Handbook*; Kadish, K. M., Smith, K. M., Guilard, R., Eds.; Academic Press: San Diego, 2000; Vol. 8, pp 115−152. (b) Fukuzumi, S.; Endo, Y.; Imahori, H. *J. Am. Chem. Soc.* **2002**, *124*, 10974.

(21) (a) Gust, D.; Moore, T. A.; Moore, A. L. *Acc. Chem. Res.* **1993**, *26*, 198. (b) Gust, D.; Moore, T. A.; Moore, A. L. *Acc. Chem. Res.* **2001**, *34*, 40. (c) Gust, D.; Moore, T. A. In *The Porphyrin Handbook*; Kadish, K. M., Smith, K. M., Guilard, R., Eds.; Academic Press: San Diego, 2000; Vol. 8, pp 153−190.

(22) (a) McDermott, G.; Prince, S. M.; Freer, A. A.; Hawthornthwaite-Lawless, A. M.; Papiz, M. Z.; Cogdell, R. J.; Isaacs, N. W. *Nature* **1995**, *374*, 517. (b) Koepke, J.; Hu, X.; Muenke, C.; Schulten, K.; Michel, H. *Structure* **1996**, *4*, 581.

(23) (a) Bar-Haim, A.; Klafter, J.; Kopelman, R. *J. Am. Chem. Soc.* **1997**, *119*, 6197. (b) Sadamoto, R.; Tomioka, N.; Aida, T. *J. Am. Chem. Soc.* **1996**, *118*, 3978. (c) Jiang, D.-L.; Aida, T. *J. Am. Chem. Soc.* **1998**, *120*, 10895. (d) Choi, M.-S.; Aida, T.; Yamazaki, T.; Yamazaki, I. *Chem. Eur. J.* **2002**, *8*, 2668.

(24) (a) Shortreed, M. R.; Swallen, S. F.; Shi, Z.-Y.; Tan, W.; Xu, Z.; Devadoss, C.; Moore, J. S.; Kopelman, R. *J. Phys. Chem. B* **1997**, *101*, 6318. (b) Gilat, S. L.; Adronov, A.; Fréchet, J. M. J. *Angew. Chem., Int. Ed.* **1999**, *38*, 1422. (c) Yeow, E. K. L.; Ghiggino, K. P.; Reek, J. N. H.; Crossley, M. J.; Bosman, A. W.; Schenning, A. P. H. J.; Meijer, E. W. *J. Phys. Chem. B* **2000**, *104*, 2596.

(25) Diederich, F.; Gömez-Löpez, M. *Chem. Soc. Rev.* **1999**, *28*, 263.

(26) Boyd, P. D. W.; Hodgson, M. C.; Rickard, C. E. F.; Oliver, A. G.; Chaker, L.; Brothers, P. J.; Bolskar, R. D.; Tham, F. S.; Reed, C. A. *J. Am. Chem. Soc.* **1999**, *121*, 10487.

(27) (a) Sun, D.; Tham, F. S.; Reed, C. A.; Chaker, L.; Burgess, M.; Boyd, P. D. W. *J. Am. Chem. Soc.* **2000**, *122*, 10704. (b) Sun, D.; Tham, F. S.; Reed, C. A.; Chaker, L.; Boyd, P. D. W. *J. Am. Chem. Soc.* **2002**, *124*, 6604. (c) Sun, D.; Tham, F. S.; Reed, C. A.; Boyd, P. D. W. *Proc. Natl. Acad. Sci. U.S.A.* **2002**, *99*, 5088.

(28) (a) Olmstead, M. M.; Costa, D. A.; Maitra, K.; Noll, B. C.; Phillips, S. L.; Van Calcar, P. M.; Balch, A. L. *J. Am. Chem. Soc.* **1999**, *121*, 7090. (b) Olmstead, M. M.; de Bettencourt-Dias, A.; Duchamp, J. C.; Stevenson, S.; Marciu, D.; Dorn, H. C.; Balch, A. L. *Angew. Chem., Int. Ed.* **2001**, *40*, 1223.

(29) (a) Tashiro, K.; Aida, T.; Zheng, J.-Y.; Kinbara, K.; Saigo, K.; Sakamoto, S.; Yamaguchi, K. *J. Am. Chem. Soc.* **1999**, *121*, 9477. (b) Zheng, J.-Y.; Tashiro, K.; Hirabayashi, Y.; Kinbara, K.; Saigo, K.; Aida, T.; Sakamoto, S.; Yamaguchi, K. *Angew. Chem., Int. Ed.* **2001**, *40*, 1857.

(30) Guldi, D. M.; Luo, C.; Prato, M.; Troisi, A.; Zerbetto, F.; Scheloske, M.; Dietel, E.; Bauer, W.; Hirsch, A. *J. Am. Chem. Soc.* **2001**, *123*, 9166.

(31) Imahori, H.; Hagiwara, K.; Aoki, M.; Akiyama, T.; Taniguchi, S.; Okada, T.; Shirakawa, M.; Sakata, Y. *J. Am. Chem. Soc.* **1996**, *118*, 11771.

(32) Wang, Y.-B.; Lin, Z. *J. Am. Chem. Soc.* **2003**, *125*, 6072.

(33) (a) Fukuzumi, S. *Pure Appl. Chem.* **2003**, *75*, 577. (b) Imahori, H.; Mori, Y.; Matano, Y. *J. Photochem. Photobiol. C* **2003**, *4*, 51.

(34) Hasobe, T.; Imahori, H.; Fukuzumi, S.; Kamat, P. V. *J. Phys. Chem. B* **2003**, *107*, 12105.

(35) (a) Imahori, H.; Yamada, K.; Yoshizawa, E.; Hagiwara, K.; Okada, T.; Sakata, Y. *J. Porphyrins Phthalocyanines* **1997**, *1*, 55. (b) Imahori, H.; Tamaki, K.; Guldi, D. M.; Luo, C.; Fujitsuka, M.; Ito, O.; Sakata, Y.; Fukuzumi, S. *J. Am. Chem. Soc.* **2001**, *123*, 2607. (c) Tkachenko, N. V.; Lemmetyinen, H.; Sonoda, J.; Ohkubo, K.; Sato, T.; Imahori, H.; Fukuzumi, S. *J. Phys. Chem. A.* **2003**, *107*, 8834.

(36) Bedja, I.; Hotchandani, S.; Kamat, P. V. *J. Phys. Chem.* **1994**, *98*, 4133.

(37) (a) Kamat, P. V.; Barazzouk, S.; Thomas, K. G.; Hotchandani, S. *J. Phys. Chem. B* **2000**, *104*, 4014 (b) Kamat, P. V.; Barazzouk, S.; Hotchandani, S.; Thomas, K. G. *Chem. Eur. J.* **2000**, *6*, 3914.

(38) Hasobe, T.; Imahori, H.; Fukuzumi, S.; Kamat, P. V. *J. Mater. Chem.* **2003**, *13*, 2515.

(39) (a) Bell, T. D. M.; Ghiggino, K. P.; Jolliffe, K. A.; Ranasinghe, M. G.; Langford, S. J.; Shephard, M. J.; Paddon-Row: M. N. *J. Phys. Chem. A* **2002**, *106*, 10079. (b) Vlassiouk, I.; Smirnov, S.; Kutzki, O.; Wedel, M.; Montforts, F.-P. *J. Phys. Chem. B* **2002**, *106*, 8657. (c) Konarev, D. V.; Kovalevsky, A. Yu.; Li, X.; Neretin, I. S.; Litvinov, A. L.; Drichko, N. V.; Slovokhotov, Y. L.; Coppens, P.; Lyubovskaya, R. N. *Inorg. Chem.* **2002**, *41*, 3638.

(40) (a) Tkachenko, N. V.; Rantala, L.; Tauber, A. Y.; Helaja, J.; Hynninen, P. H.; Lemmetyinen, H. *J. Am. Chem. Soc.* **1999**, *121*, 9378. (b) Kesti, T. J.; Tkachenko, N. V.; Vehmanen, V.; Yamada, H.; Imahori, H.; Fukuzumi, S.; Lemmetyinen, H. *J. Am. Chem. Soc.* **2002**, *124*, 8067.

(41) (a) Imahori, H.; Sakata, Y. *Adv. Mater.* **1997**, *9*, 537. (b) Imahori, H. *J. Phys. Chem. B* **2004**, *108*, 6130.

(42) Guldi, D. M.; Prato, M. *Acc. Chem. Res.* **2000**, *33*, 695.

(43) Guldi, D. M. *Chem. Commun.* **2000**, 321.

(44) (a) Fukuzumi, S.; Hasobe, T.; Endo, Y.; Kei Ohkubo, K.; Imahori, H. *J. Porphyrins Phthalocyanines* **2003**, *7*, 328. (b) Fukuzumi, S.; Nakanishi, I.; Suenobu, T.; Kadish, K. M. *J. Am. Chem. Soc.* **1999**, *121*, 3468.